

Synthesis and Characterization of F/Mn Co-doped SnO₂ Nanoparticles by Hydrothermal Method

Wu Zhijun¹, Zheng Weimeng¹, Wang Junsheng¹, Tang Sha², Li Wenya³, Lv Weizhong¹

¹ Shenzhen University, Shenzhen 518060, China; ² Shenzhen Dawei Nano Technology Co. Ltd, Shenzhen 518172, China; ³ National Taipei University of Technology, Taipei 10697, China

Abstract: F-Mn co-doped SnO₂ nanoparticles with rutile structure were synthesized by hydrothermal method. Effects of alkali source, pH, dopant, surfactant, and calcination temperature on crystalline phases, micromorphology, dispersion, and optical properties of F/Mn co-doped SnO₂ nanoparticles were studied. The F-Mn co-doped SnO₂ nanoparticles were characterized by X-ray diffraction (XRD), scanning electron microscopy (SEM) and ultraviolet/visible/near (UV-Vis-NIR) spectrophotometer. The results show that we can get F-Mn co-doped SnO₂ nanoparticles with higher crystallinity, smaller diameters and well dispersion. The F-Mn co-doped SnO₂ coating has a good lighting and high near-infrared shielding performance, in which the transmittance of visible light is about 90% and the near-infrared shielding rate is about 93%.

Key words: F/Mn co-doped SnO₂; hydrothermal; near-infrared shielding

Tin dioxide (SnO₂) is an n-type semiconductor with a wide band gap of $E_g=3.6\sim 4.0$ eV^[1,2], showing high chemical and mechanical stabilities. SnO₂ possesses superior properties and is widely used in various fields, such as catalyst, conductive ceramics, sensors, displays, solar cells, and optical. Thus, tin dioxide is widely used in thermal insulation coatings. Many scholars have studied the different element doped tin dioxides, such as Yb-doped SnO₂, Ni-doped SnO₂, Mn-doped SnO₂, La-doped SnO₂, and Cu-doped SnO₂^[3-7], used in conductive ceramics, sensors, displays, solar cells, optical, etc. Several methods have been applied to synthesize SnO₂ nano-materials, such as thermal evaporation^[8], plasma treatment^[9], laser ablation^[10], hydrothermal^[11,12], solvothermal^[13], precipitation^[14,15], microemulsion^[16] and sol-gel^[17].

In the present study, hydrothermal method was used to prepare F/Mn co-doped SnO₂ powder. The effects of alkali source, pH, dopant, surfactant, and calcination temperature on crystalline phases, micromorphology, dispersion, and optical properties of F/Mn co-doped SnO₂ were investigated. The

hydrothermal method is a simple, cost-effective, non-polluting and energy saving process, so it is suitable for industrial production. The products synthesized by the hydrothermal method are of high purity, well-dispersibility and controllable sizes.

1 Experiment

All reagents were of analytical grade without any further purification. In a typical procedure, appropriate amounts of oxalic acid (C₂H₂O₄·2H₂O) were dispersed into 50 mL de-ionized water with magnetic stirring for about 10 min at the room temperature to adjust pH value to about 2. The purpose is to inhibit the hydrolysis of tin (IV) chloride pentahydrate (SnCl₄·5H₂O) too quickly. 8.765 g SnCl₄·5H₂O and appropriate amounts of ammonium fluoride (NH₄F), potassium fluoride (KF), hydrofluoric acid (HF), sodium fluoride (NaF) as well as manganese (II) chloride tetrahydrate (MnCl₂·4H₂O), manganese (II) sulfate monohydrate (MnSO₄·H₂O) were then added to the oxalic acid solution. After continuously stirring

Received date: June 4, 2019

Foundation item: Research & Development Fund of Guangdong (2016B090930011); Research & Development Fund of Shenzhen City (JCYJ20160226192609015, GJHZ20180929110606770)

Corresponding author: Lv Weizhong, Ph. D., Professor, College of Chemistry and Environmental Engineering, Shenzhen University, Shenzhen 518060, P. R. China, Tel: 0086-755-26557249, E-mail: lvwzh@szu.edu.cn

Copyright © 2020, Northwest Institute for Nonferrous Metal Research. Published by Science Press. All rights reserved.

for 1 h, the suspension was added with 0.5 mmol of polyethylene glycol (PEG) (for structural units), sodium stearate, sodium dodecyl sulfonate (SDS), tetrapropylammonium bromide (TPAB) or cetyltrimethyl ammonium bromide (CTAB) and ultrasonically dispersed for 0.5 h. Then NaOH solution, potassium hydroxide (KOH) and ammonium hydroxide ($\text{NH}_3\cdot\text{H}_2\text{O}$) were slowly dropped into the SnCl_4 solution until the pH value reached 6~11 under continuous magnetic stirring and a brown suspended solution was obtained, which was then transferred into a Teflon-lined autoclave (100 mL), and held in an electric oven at 200 °C for 12 h. Finally the autoclave was allowed to cool to room temperature naturally. The brown powder was harvested by filtration and washed with de-ionized water several times before drying in vacuum at 100 °C for 3 h.

The prepared F-Mn co-doped SnO_2 nanoparticles were dispersed in water, and then mixed with polycarbonate and a proper amount of additives to prepare coating. The coating was sprayed on the glass sheet and dried to get the thin film.

2 Results and Discussion

X-ray diffraction (XRD) analysis was used to examine the crystal structure of the products. The patterns of F-Mn co-doped SnO_2 nanosized powders synthesized with different alkali source are shown in Fig.1. Fig.1c shows that the XRD peaks of F-Mn co-doped SnO_2 prepared with $\text{NH}_3\cdot\text{H}_2\text{O}$ as alkali source are not much sharper. Fig.1b shows that the XRD pattern of F-Mn co-doped SnO_2 prepared with KOH as alkali source agrees with the standard JCPDS card No.01-0657. Fig.1a shows that the XRD pattern of F-Mn co-doped SnO_2 prepared with NaOH as alkali source agrees well with the standard data and the strong and sharp peaks indicate that the F-Mn co-doped SnO_2 nanosized powders are highly crystallized.

The XRD patterns of F-Mn co-doped SnO_2 nanoparticles synthesized with different pH are shown in Fig.2. It shows that rutile phases F-Mn co-doped SnO_2 crystallites with

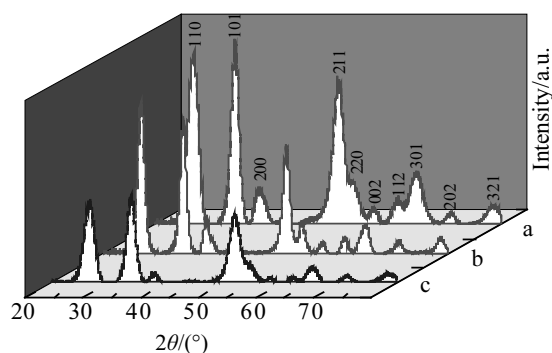


Fig.1 XRD patterns of F-Mn co-doped SnO_2 ($\text{F}_{0.05}\text{Mn}_{0.05}\text{Sn}_{0.90}\text{O}_2$) nanosized powders synthesized by different alkali source: (a) NaOH, (b) KOH, and (c) $\text{NH}_3\cdot\text{H}_2\text{O}$

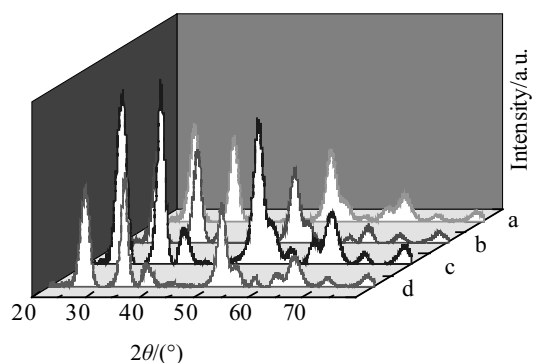


Fig.2 XRD patterns of F-Mn co-doped SnO_2 ($\text{F}_{0.05}\text{Mn}_{0.05}\text{Sn}_{0.90}\text{O}_2$) nanosized powders synthesized with different pH: (a) pH=6, (b) pH=8, (c) pH=10, and (d) pH=11

tetragonal structure could be directly obtained with different pH.

Furthermore, the crystallite grain size of F-Mn co-doped SnO_2 could be estimated as 8~10 nm according to Scherrer formula $L=K\lambda/\beta\cos\theta$, where $K=0.89$ is a constant, $\lambda=0.154056$ nm is X-ray wavelength, β is FWHM, θ is Bragg's angle in degree. When pH=10, the peaks are strongest. The condition of the pH=10 is probably most conducive to the crystals. The XRD patterns of F-Mn co-doped SnO_2 nanosized powders synthesized with different dopants are shown in Fig.3. No impurity peaks are observed, indicating the high purity of the final products.

The product morphology was determined by scanning electron microscopy (SEM). SEM images of F-Mn co-doped SnO_2 prepared with different alkali source are shown in Fig.4. Fig.4c shows that the morphology of F-Mn co-doped SnO_2 prepared with $\text{NH}_3\cdot\text{H}_2\text{O}$ as alkali source likes a similar mesh

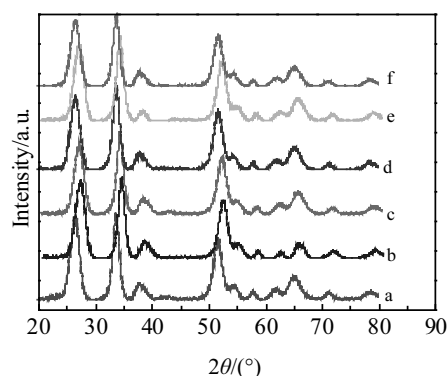


Fig.3 XRD patterns of F-Mn co-doped SnO_2 ($\text{F}_{0.05}\text{Mn}_{0.05}\text{Sn}_{0.90}\text{O}_2$) nanosized powders synthesized with different dopants: (a) NH_4F & $\text{MnCl}_2\cdot 4\text{H}_2\text{O}$, (b) HF & $\text{MnSO}_4\cdot\text{H}_2\text{O}$, (c) $\text{KFMnCl}_2\cdot 4\text{H}_2$, (d) KF & $\text{MnSO}_4\cdot\text{H}_2\text{O}$, (e) NaF & $\text{MnCl}_2\cdot 4\text{H}_2\text{O}$, and (f) NaF & $\text{MnSO}_4\cdot\text{H}_2\text{O}$

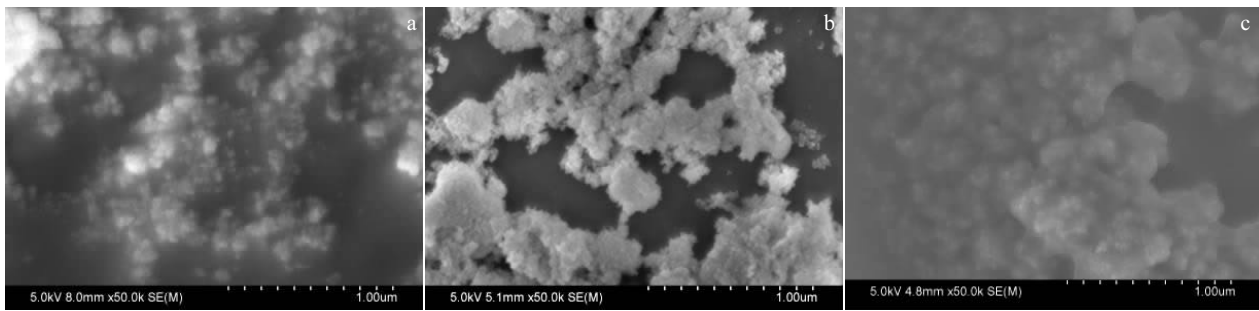


Fig.4 SEM images of F-Mn co-doped SnO_2 ($\text{F}_{0.05}\text{Mn}_{0.05}\text{Sn}_{0.90}\text{O}_2$) prepared with different alkali source: (a) NaOH, (b) KOH, and (c) $\text{NH}_3\cdot\text{H}_2\text{O}$

composed of nanoparticles. Fig.4b shows that the morphology of F-Mn co-doped SnO_2 prepared with KOH as alkali source likes snowflake composed of nanoparticles. Fig.4a shows that the morphology of F-Mn co-doped SnO_2 prepared with NaOH as alkali source shows irregular nanoparticles with good dispersion.

SEM images of F-Mn co-doped SnO_2 prepared with different surfactants are shown in Fig.5. Fig.5a shows the morphology of the products obtained without surfactant. Fig.5b~5f shows the morphologies of the products obtained with different surfactants while keeping other experimental conditions unchanged. Fig.5a shows that the sample without surfactant is severely agglomerated. The morphology of the product prepared with CTAB shows the best particle size distribution and the good dispersion.

SEM images of the F-Mn co-doped SnO_2 prepared at

different calcination temperatures are shown in Fig.6. The calcination temperature has more influence on the morphology of nanoparticles. The morphology of F-Mn co-doped SnO_2 obtained at $600\text{ }^\circ\text{C}$ (Fig.6a) shows uniform particles with polyhedron structure. Fig.6b and 6c show that the polyhedron structure disappears into nanoparticles, when the calcination temperature is 700 or $800\text{ }^\circ\text{C}$. The morphology of F-Mn co-doped SnO_2 obtained at $900\text{ }^\circ\text{C}$ (Fig.6d) shows uniform particles with bigger polyhedron structure. The mechanism may be the crystal melting at 700 and $800\text{ }^\circ\text{C}$, and the formation of bigger crystallization with the calcination temperature at $900\text{ }^\circ\text{C}$.

The ultraviolet/visible/near-infrared transmission spectra of blank glass and the glass coated with F-Mn co-doped SnO_2 film are shown in Fig.7. Blank glass has high visible light transmittance, but almost no near infrared shielding effect.

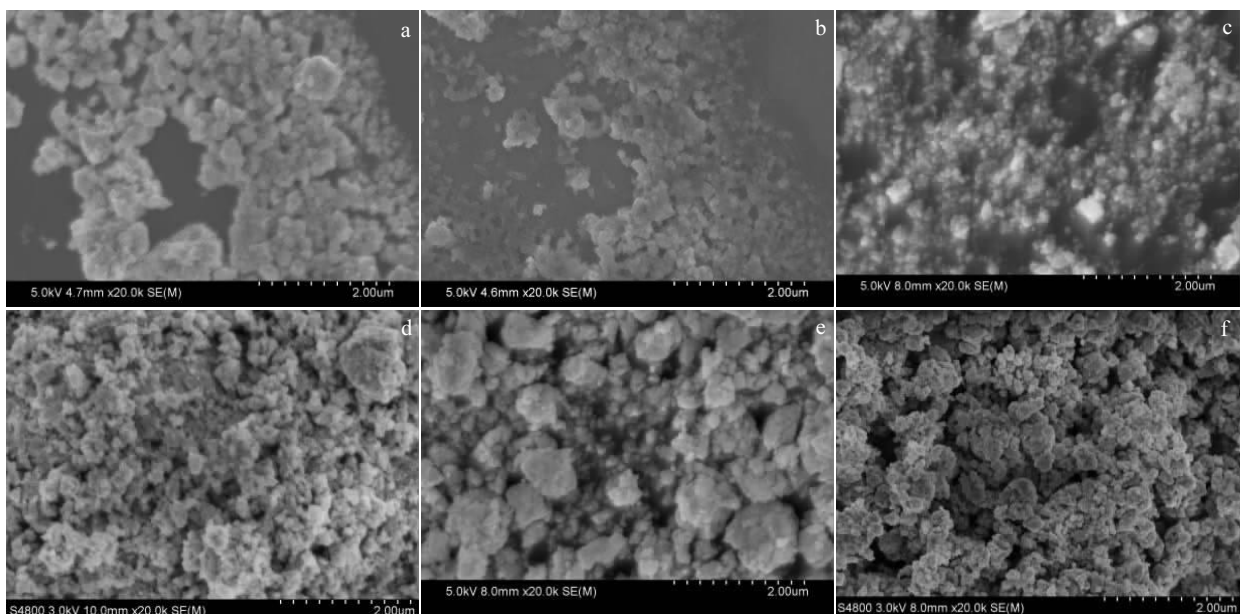


Fig.5 SEM images of F-Mn co-doped SnO_2 ($\text{F}_{0.05}\text{Mn}_{0.05}\text{Sn}_{0.90}\text{O}_2$) prepared with different surfactants: (a) no surfactant, (b) PEG, (c) CTAB, (d) SDS, (e) sodium stearate, and (f) TPAB

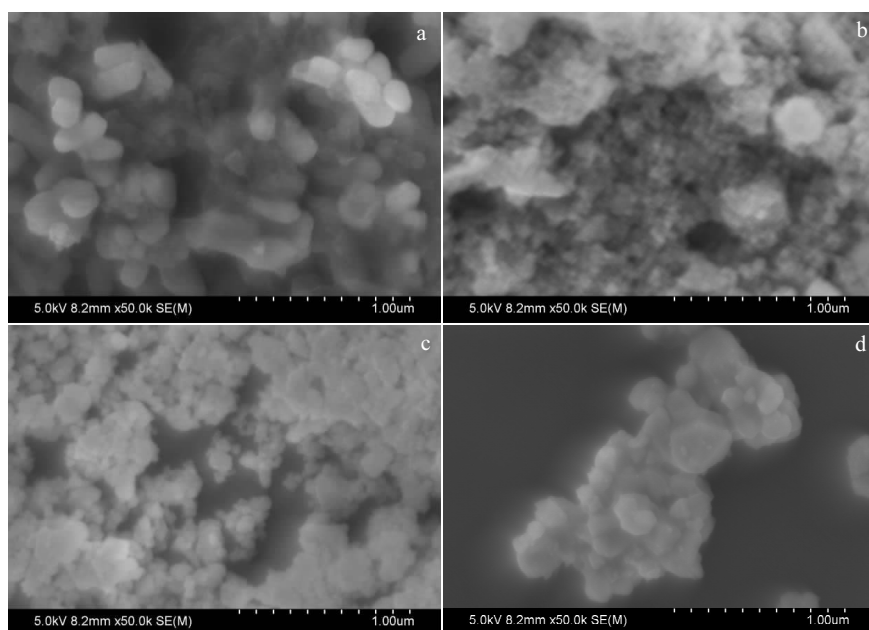


Fig.6 SEM images of F-Mn co-doped SnO_2 ($\text{F}_{0.05}\text{Mn}_{0.05}\text{Sn}_{0.90}\text{O}_2$) prepared by a typical hydrothermal method at different calcination temperatures: (a) 600 °C, (b) 700 °C, (c) 800 °C, and (d) 900 °C

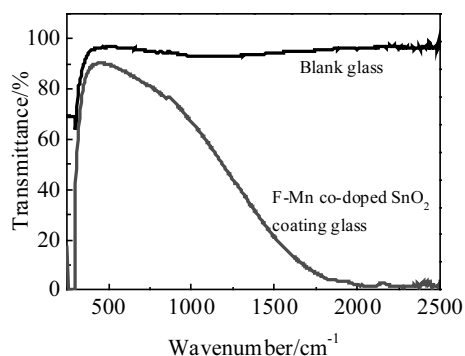


Fig.7 UV-Vis-NIR transmission spectra of blank glass and the glass coated with F-Mn co-doped SnO_2 ($\text{F}_{0.05}\text{Mn}_{0.05}\text{Sn}_{0.90}\text{O}_2$) film

The coated glass maintains a high visible light transmittance and has strong near-infrared shielding effect in 1500~2500 cm^{-1} . The transmittance of visible light is about 90% and the near-infrared shielding rate is about 93%. It indicates that the F-Mn co-doped SnO_2 film has good daylighting and strong near-infrared shielding performance.

3 Conclusions

1) A simple hydrothermal process to synthesize F-Mn co-doped SnO_2 ($\text{F}_{0.05}\text{Mn}_{0.05}\text{Sn}_{0.90}\text{O}_2$) nanocrystals with higher crystallinity, smaller diameters, well dispersion and good optical performance was demonstrated. All the synthesized SnO_2 are of tetragonal crystal structure with different dopants

and pH. Different surfactants, alkali source and calcination temperatures influence the morphology of nanocrystals.

2) The F-Mn co-doped SnO_2 coating has a good lighting and high near-infrared shielding performance, in which the transmittance of visible light is about 90% and the near-infrared shielding rate is about 93%.

References

- Bandara J, Divarathne C M, Nanayakkara S D. *Solar Energy Materials and Solar Cells*[J], 2004, 81(4): 429
- Kirschbaum F, Schugardt C. *Journal of Physiology-Paris*[J], 2002, 96(5-6): 557
- Sharma S, Shah J, Kotnala R K et al. *Electronic Materials Letters*[J], 2013, 9(5): 615
- Sharma A, Varshney M, Kumar S et al. *Nanomaterials and Nanotechnology*[J], 2011, 1(1): 29
- Liu L, Zhang T, Wang L Y et al. *Materials Letters*[J], 2009, 63(23): 2041
- Wang J B, Liu Y, Fu C et al. *Rare Metal Materials and Engineering*[J], 2009, 38(11): 2023 (in Chinese)
- Fitzgerald C B, Venkatesan M, Douvalis A P et al. *Journal of Applied Physics*[J], 2004, 95(11): 7390
- Dai Z R, Pan Z W, Wang Z L. *Journal of the American Chemical Society*[J], 2002, 124(29): 8673
- Meduri P, Pendyala C, Kumar V et al. *Nano letters*[J], 2009, 9(2): 612
- Hu J Q, Bando Y, Liu Q L et al. *Advanced Functional Materials*[J], 2003, 13(6): 493
- Karunakaran C, Raadha S S, Gomathisankar P. *Journal of Alloys*

- and Compounds[J], 2013, 549: 269
- 12 Kakati N, Maiti J, Jee S H et al. *Journal of Alloys and Compounds*[J], 2011, 509(18): 5617
- 13 Rashad M M, Ismail A A, Osama I et al. *Arabian Journal of Chemistry*[J], 2014, 7(1): 71
- 14 Bastami H, Taheri-Nassaj E. *Journal of Alloys and Compounds*[J], 2010, 495(1): 121
- 15 Xu M H, Cai F S, Yin J et al. *Sensors and Actuators B: Chemical*[J], 2010, 145(2): 875
- 16 Xi L J, Qian D, Huang X H et al. *Journal of Alloys and Compounds*[J], 2008, 462(1): 42
- 17 Mazloom J, Ghodsi F E, Gholami M. *Journal of Alloys and Compounds*[J], 2013, 579: 384

水热法制备 F/Mn 共掺杂 SnO₂ 纳米粒子的合成与表征

吴志军¹, 郑威猛¹, 王俊生¹, 唐莎², 李文亚³, 吕维忠¹

(1. 深圳大学, 广东 深圳 518060)

(2. 深圳市大维纳米科技有限公司, 广东 深圳 518172)

(3. 台北科技大学, 台湾 台北 10697)

摘要: 采用水热法制备了具有金红石结构的 F-Mn 共掺杂 SnO₂ 纳米粒子, 研究了碱源、pH 值、掺杂剂、表面活性剂、煅烧温度对 F/Mn 共掺杂 SnO₂ 纳米粒子晶相、微观形貌、分散性和光学性能的影响。采用 X 射线衍射 (XRD)、扫描电镜 (SEM) 和紫外/可见/近红外分光光度计对 F-Mn 共掺杂 SnO₂ 纳米粒子进行了表征。结果表明, 该方法可以获得较高的结晶度、较小的粒径和分散良好的 F-Mn 共掺杂 SnO₂ 纳米粒子。F-Mn 共掺杂 SnO₂ 涂层具有较好采光的同时有较好的近红外屏蔽性能, 其中可见光透过率约为 90%, 近红外阻隔率约为 93%。

关键词: F/Mn 共掺杂 SnO₂; 水热; 近红外屏蔽

作者简介: 吴志军, 男, 1991 年生, 博士生, 深圳大学化学与环境工程学院, 广东 深圳 518060, 电话: 0755-26557249, E-mail: 1248575486@qq.com